ELSEVIER

Carbohydrate Research 256 (1994) 223–244

CARBOHYDRATE RESEARCH

Involvement of the glucose moiety in the molecular recognition of methyl β-lactoside by ricin: synthesis, conformational analysis, and binding studies of different derivatives at the C-3 region.

P. Fernández [a], J. Jiménez-Barbero [a], M. Martín-Lomas [a], D. Solís [b], T. Díaz-Mauriño [b]

[a] *Grupo de Carbohidratos, Instituto de Química Orgánica General, C.S.I.C., Juan de la Cierva 3, 28006 Madrid, Spain* [b] *Instituto de Química Física "Rocasolano", C.S.I.C., Serrano 119, 28006 Madrid, Spain*

(Received May 14th, 1993; accepted September 29th, 1993)

Abstract

Syntheses of the 3-aminodeoxy (**4**), 3-deoxy-3-methyl (**5**), and 3-epi (**6**) derivatives of methyl β-lactoside (**1**) have been achieved from **1** in a straightforward way, and their solution conformations in water and dimethyl sulfoxide analysed through molecular mechanics and dynamics calculations and nuclear magnetic resonance data. The overall shape of all the compounds studied is fairly similar and may be described by conformers included in a low energy region with $\Phi = 15 \pm 45°$ and $\Psi = -25 \pm 30°$, that is ca. 5% of the total potential energy surface for the glycosidic linkages of the disaccharides. The binding of the different compounds to ricin, the galactose-specific toxin from *Ricinus communis*, has been investigated. The results confirm the involvement of the C-3 region in a nonpolar interaction with the protein at the periphery of the combining site.

1. Introduction

The use of engineered ligands is a practical approach to probe the combining sites of proteins of biological interest. The study of the recognition phenomenon based on modified substrates must be accompanied by analysis of the possible changes in their three-dimensional structure in order to be able to correlate structure and activity.

We have previously investigated the molecular recognition of methyl β-lactoside (**1**) and its monodeoxy derivatives by the β-galactoside-specific lectins isolated from *Ricinus communis* seeds, ricin and agglutinin [1,2]. Binding of methyl β-

0008-6215/94/$07.00
SSDI 0008-6215(93)E0381-A

lactoside to ricin B-chain results in only a small change in the disaccharide geometry [3], which probably represents the selection of one conformer of the range of those existing in solution. As determined by NMR and molecular mechanics calculations [1], the preferred conformations of the different methyl β-lactoside derivatives were very similar. Therefore, the relative affinity of the lectins for the different structures could be correlated with specific polar and nonpolar interactions. Thus, the hydroxyl groups at positions 3, 4, and 6 of the D-galactopyranose moiety are key polar groups and the hydroxyl group at position 2 of this unit plays a minor role. In addition, the $^4C_1$ conformation of the D-glucopyranose moiety of methyl β-lactoside is important for the recognition and binding. A nonpolar interaction involving the C-3 region can be predicted from the results obtained for the 3-deoxy (**2**) and 3-*O*-methyl (**3**) derivatives [1].

However, the involvement of ligand residues beyond the terminal galactose in binding to ricin is a matter of controversy. Though lactose is a more effective inhibitor of the lectin than galactose, no specific interactions of the glucose moiety with the protein are observed in the 0.25-nm X-ray crystal structure of the ricin–lactose complex [4]. Similarly, a crystal structure of a biantennary oligosaccharide with ricin shows only the same galactose contacts with the protein [4], notwithstanding that the lectins bind 1000-fold better to oligosaccharides with terminal galactosides than to simple sugars [5]. In addition, in a recent report on the conformation of methyl β-melibioside bound to ricin B-chain [6], no particularly important interactions seem evident for the glucose ring, although favorable hydrophobic contacts at one of the two binding sites present in ricin B-chain, the C-terminal or high affinity site, can be predicted from docking studies on the allowed conformers.

In order to clarify the role of the glucose moiety in the molecular recognition of methyl β-lactoside by ricin, we have synthesized several derivatives with different features at the C-3 position, namely, the 3-amino-3-deoxy (**4**), the 3-deoxy-3-methyl (**5**), and the 3-epi (**6**) analogues of methyl β-lactoside (**1**). Quantitative binding studies coupled with conformational analysis of free ligands in solution confirms the existence of a nonpolar interaction of this region with the lectin surface.

2. Results and discussion

Synthesis.—A suitable compound with position O-3 differentiated from the remaining hydroxyl groups was necessary for the synthesis of **4–6** We reported [2] that methyl 2,6,2′,3′,4′,6′-hexa-*O*-benzyl-β-lactoside (**7**, 43%) can be obtained easily from methyl β-lactoside (**1**) by partial benzylation under phase-transfer conditions. Therefore, **7** was used for the syntheses of the 3-amino-3-deoxy (**4**), 3-deoxy-3-methyl (**5**), and 3-epi (**6**) analogues of **1**.

Swern oxidation of **7** led to ketone **8** (67%), which gave the corresponding *O*-benzyloxime (**9**, 84%). Reduction of **9** with lithium aluminum hydride in ether yielded the desired **10** (43%), along with the analogue with an axial 3-NH_2 group (**11**, 25%). Conventional hydrogenolysis of **10** afforded **4** (90%).

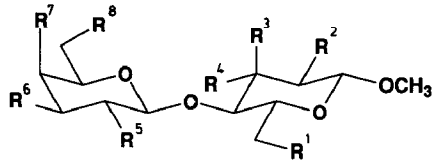

1 $R^1 = R^2 = OH$, $R^3 = H$, $R^4 - R^8 = OH$
2 $R^1 = R^2 = OH$, $R^3 = R^4 = H$, $R^5 - R^8 = OH$
3 $R^1 = R^2 = OH$, $R^3 = H$, $R^4 = OCH_3$, $R^5 - R^8 = OH$
4 $R^1 = R^2 = OH$, $R^3 = H$, $R^4 = NH_2$, $R^5 - R^8 = OH$
5 $R^1 = R^2 = OH$, $R^3 = H$, $R^4 = CH_3$, $R^5 - R^8 = OH$
6 $R^1 = R^2 = OH$, $R^3 = OH$, $R^4 = H$, $R^5 - R^8 = OH$

7 $R^1 = R^2 = OBn$, $R^3 = H$, $R^4 = OH$, $R^5 - R^8 = OBn$
8 $R^1 = R^2 = OBn$, $R^3, R^4 = O$, $R^5 - R^8 = OBn$
9 $R^1 = R^2 = OBn$, $R^3, R^4 = N\text{-}OBn$, $R^5 - R^8 = OBn$
10 $R^1 = R^2 = OBn$, $R^3 = H$, $R^4 = NH_2$, $R^5 - R^8 = OBn$
11 $R^1 = R^2 = OBn$, $R^3 = NH_2$, $R^4 = H$, $R^5 - R^8 = OBn$
12 $R^1 = R^2 = OBn$, $R^3, R^4 = CH_2$, $R^5 - R^8 = OBn$
13 $R^1 = R^2 = OBz$, $R^3 = H$, $R^4 = CH_3$, $R^5 - R^8 = OBz$
14 $R^1 = R^2 = OBn$, $R^3 = OAc$, $R^4 = H$, $R^5 - R^8 = OBn$

The 3-*C*-methyl analogue was prepared following the strategy of Magnusson and co-workers [7]. Wittig reaction of ketone **8** with methylenetriphenylphosphorane gave **12** (51% allowing for recovered starting material). Hydrogenation and hydrogenolysis of **12** afforded a mixture (85:15) of the two epimers at C-3. The desired compound with an equatorial methyl group could be crystallized from methanol as the corresponding hexabenzoate **13**; Zemplén deacylation produced pure **5** (95%).

The 3-epi analogue (*allo* configuration) was obtained by S_N2 inversion of the trifluoromethanesulfonate of **7**. Treatment of this compound with sodium nitrite [8] in DMF at room temperature furnished a mixture of products. On the other hand, reaction of the triflate with tetrabutylammonium acetate in toluene [9] afforded **14** (68%). Hydrogenolysis and Zemplén deacylation gave **6** (89%).

Conformational analysis.—Table 1 shows the values of the estimated populations of the different conformers of **4–6** obtained by MM2 optimisation of the HSEA minima obtained previously [1] for **1**, along with those obtained by use of the Discover-CVFF and Discover-AMBER programmes [10]. The calculated energies should be taken as approximate since they are variable by at least 0.5 kcal/mol. Fig. 1 shows views of the low energy conformers and their corresponding Φ and Ψ values. According to the calculations, and independently of the force field, the low energy region is described by $\Phi = 15 \pm 45°$, $\Psi = -25 \pm 30°$, and $r_{H\text{-}1'\text{-}H\text{-}4} = 2.4 \pm 0.4$ Å, and appears to be populated to an extent of more than 90%, while the two islands described by conformers **D** and **E** are populated less than 10% at 37° or 60°. Nevertheless, the possibility of their existence in solution should be investigated since the conformation of some synthetic interglycosidic acetals of lactose and cellobiose [11] is that of conformer **D**. Very recently, an X-ray analysis of the bound conformation of a biantennary octasaccharide to

Table 1
Estimated Populations (%) for the low energy conformers of **4–6**, calculated from the MM2 [a], CVFF [b], and AMBER [c] steric energy values

Compound	Conformer				
	A	**B**	**C/C'** [d]	**D**	**E**
	Pop	Pop	Pop	Pop	Pop
4	32.9 [a]	37.8	25.3	2.9	1.1
	36.5 [b]	30.8	30.7	1.8	0.2
	38.7 [c]	28.8	23.5	0.7	8.3
5	46.5 [a]	35.5	16.0	1.6	0.4
	61.6 [b]		36.9	1.3	0.2
	63.9 [c]		26.1	1.8	8.2
6	36.0 [a]	32.3	29.7	1.7	0.3
	38.8 [b]	27.7	31.6	1.5	0.4
	[c]	58.0	38.5	2.3	1.2

[a] From MM2 energy values. [b] From CVFF energy values. [c] From AMBER energy values. [d] Minimum **C** shows *gt* orientation for the C-5–C-6 torsion angle of the glucopyranose ring, while conformer **C'** shows *gg* orientation for the C-5–C-6 torsion angle of the glucopyranose ring.

Lathyrus ochrus Isolectin I has shown the presence of a β-Man-(1 → 4)-GlcNAc linkage in conformation **E**, and a β-Gal-(1 → 4)-GlcNAc moiety located in island **D** [12]. Our results for **4–6** are in agreement with those obtained for different equatorial-linked β-(1 → 4) disaccharides, using different force fields. The stability of the different conformations was tested by molecular dynamics simulations (MD) using the Discover-CVFF and Discover-AMBER programs. Although these are general MD programs not specifically parametrized for oligosaccharides [13], and therefore do not include any potential for the anomeric effects, their use in the conformational analysis of different oligosaccharides has produced satisfactory results [14]. The minimized **A–E** conformations were used as input geometries for different 1-ns simulations at 303 K. Some typical trajectories are displayed in Fig. 2. No chair-to-chair or chair-to-boat interconversions were observed. The average Φ and Ψ angles were $35 \pm 15°$ and $-10 \pm 15°$ depending on the starting conformation. After the corresponding equilibration periods (20–120 ps), it can be observed that the simulations remained most of the time (> 90%) in the low energy region described by conformers **A–C**. In fact, only when the simulation started from geometries **D** or **E** was there significant occupancy of these islands for ca. 100–200 ps, although the trajectory went again to the broad low-energy region. Therefore, these results seem to indicate that conformers **D** and **E** are not stable enough to compete with **A–C**, when such external factors as stabilization by hydrogen or covalent bonds or nonpolar contacts are not operating [12]. In all cases, several transitions between the *gg*, *gt*, and *tg* orientations of the lateral chains were observed.

NMR spectroscopy can be used either qualitatively or quantitatively to distinguish the presence of either conformer [15]. The different interatomic distances that are susceptible to verification by NMR methodology are collected in Table 2.

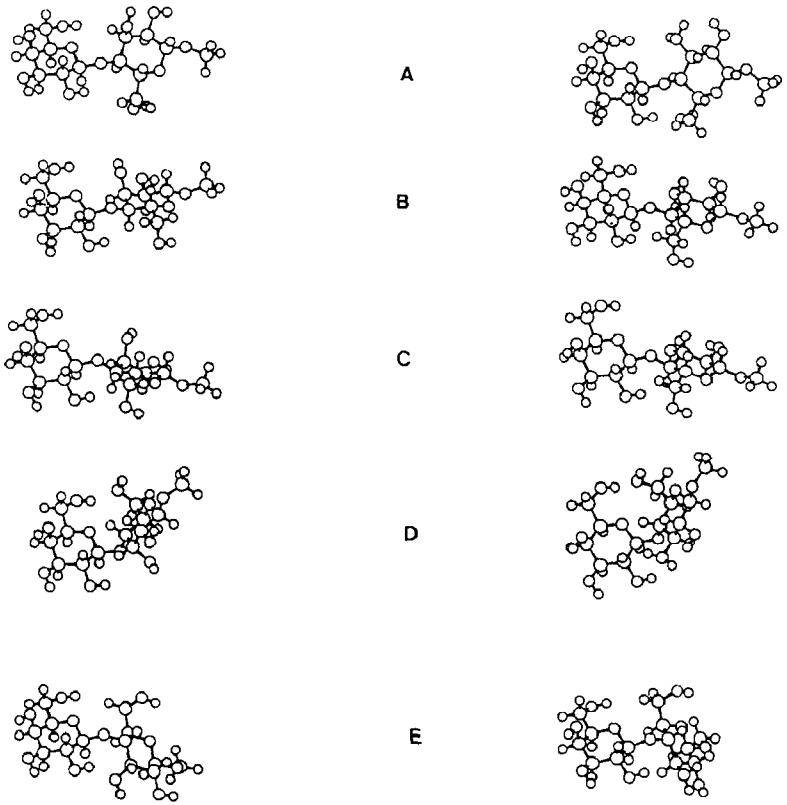

Fig. 1. Views of the low-energy conformers of **4** and **5** according to the MM2, AMBER, and CVFF programmes: **A**, Φ 50°, Ψ 4°; **B**, Φ 30°, Ψ −50°; **C**, Φ −30°, Ψ −30°; **D**, Φ 180°, Ψ −5°; **E**, Φ 40°, Ψ 180°.

It is well known that the observation of one or two interresidue NOEs and some specific shieldings or deshieldings impose constraints in the conformational map, indicating the presence of a given conformer [15,16]. The first step in the protocol always involves the unambiguous assignment of all the resonance signals, which was completed by combination of homo- and hetero-2D-NMR techniques. The first-order chemical shifts and relevant coupling constants for **1** and **4–6** are shown in Tables 3–5.

No important chemical shift differences were detected between **1** and **4–6** in D_2O or Me_2SO-d_6 solutions, apart from those expected for specific substitution. The ^1H NMR chemical shifts for the hydroxyl and amino protons in methyl sulfoxide at 30°C and the differences between these values and those determined at 50 and 70°C (data not shown) did not indicate the presence of any intramolecular hydrogen bonding as was observed [17] between HO-3 and O-5′ in **1**.

Hydroxymethyl conformation.—After assignment of the glucose and galactose H-6_{proR} and H-6_{proS} as previously reported for similar derivatives [18], the distri-

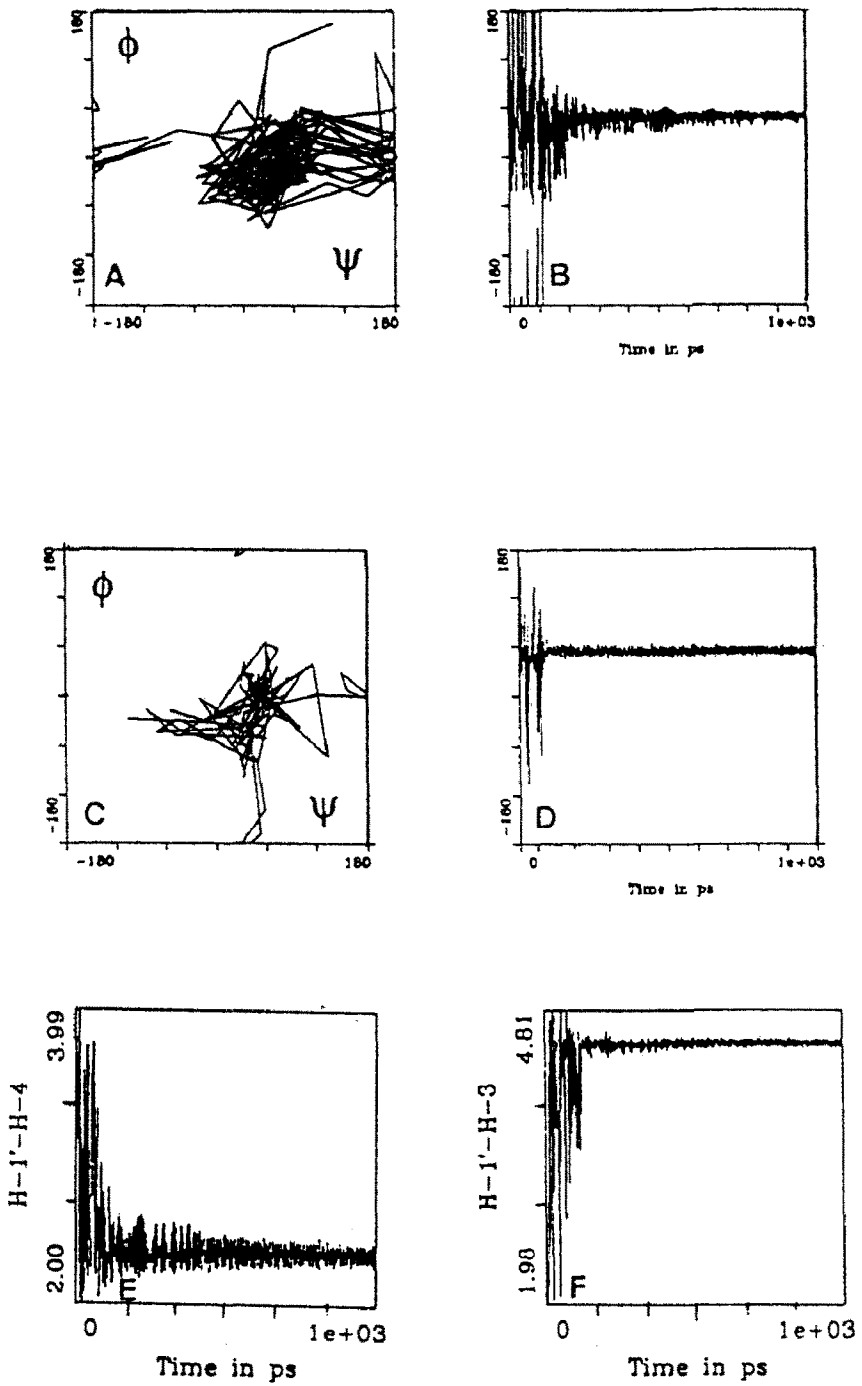

Fig. 2. A, Contour plot of the of the trajectory (1 ns) calculated by the CVFF programme for compound **5** at 303 K, starting from coordinates corresponding to conformer **D**. B, History of Φ angle for the same trajectory. C, Contour plot of the trajectory (1 ns) calculated by the CVFF programme for compound **6** at 303 K, starting from coordinates corresponding to conformer **C**. D, History of Φ angle for the same trajectory. E, History of the distance between H-1′ and H-4 for a trajectory started from coordinates of conformer **E** of compound **4**. F, History of the distance between H-1′ and H-3 for the same trajectory.

Table 2
Relevant interatomic distances for the low energy conformers of **4–6**

Distance (Å)	Conformer (Φ/Ψ)				
	A 50/4	**B** 30/−55	**C** −30/−30	**D** 180/5	**E** 35/180
H-1′–H-4	2.33	2.34	2.23	> 3.5	> 3.5
H-1′–H-3 [c]	> 3.5	> 3.5	> 3.5	> 3.5	1.79
H-1′–H-5	> 3.5	> 3.5	> 3.5	> 3.5	2.23
H-1′–H-6_R	2.49 [a]	> 3.5	> 3.5	> 3.5	> 3.5
H-1′–H-6_S	2.62 [b]	> 3.5	> 3.5	> 3.5	> 3.5
H-1′–X-3 [d]	> 3.5	2.48	2.47	> 3.5	> 3.5
H-1′–O-6	2.52	> 3.5	> 3.5	> 3.5	> 3.5
H-2′–H-4	> 3.5	> 3.5	> 3.5	1.94	> 3.5
O-2′–X-3 [d]	> 3.5	> 3.5	> 3.5	2.93	> 3.5
O-5′–X-3 [d]	3.02	2.63	3.06	> 3.5	> 3.5
O-2′–H-6_R	2.96 [a]	> 3.5	3.12	> 3.5	> 3.5
O-2′–H-6_S	2.99 [b]	> 3.5	3.06	> 3.5	> 3.5

[a] *gg* or [b] *gt* rotamers around the C-5–C-6 bond. [c] H-3 and O-3 are interchanged for compound **6**. [d] X stands for N(**4**), C(**5**), or O(**6**).

bution of rotamers was calculated for those compounds which showed resolved couplings for H-5 (Table 5) and/or the corresponding H-6's, following well-established methodology [19] by using the Karplus–Altona [20] equation. The observed couplings for the lateral chain of the different glucose residues are consistent with

Table 3
^{1}H NMR chemical shifts (δ, ppm) for compounds 1 and **4–6** in D_2O and Me_2SO-d_6 solution at 37°C

Proton	Compound							
	1 [a]	**4** [a]	**5** [a]	**6** [a]	**1** [b]	**4** [b]	**5** [b]	**6** [b]
Glucose residue								
H-1	4.40	4.48	4.36	4.62	4.09	4.26	4.03	4.36
H-2	3.30	3.51	3.08	3.45	3.00	3.46	2.76	3.10
H-3	3.64	3.38	1.72	4.41	3.32	3.02	1.42	4.04
H-4	3.63	3.95	3.50	3.77	3.44	3.74	3.22	3.43
H-5	3.59	3.71	3.60	3.88	3.38	3.41	3.23	3.61
H-6_S	3.98	3.99	4.03	3.95	3.74	3.91	3.71	3.70
H-6_R	3.80	3.83	3.76	3.76	3.61	3.64	3.59	3.56
Galactose residue								
H-1′	4.44	4.48	4.41	4.47	4.19	4.26	4.17	4.21
H-2′	3.53	3.56	3.51	3.54	3.32	3.34	3.25	3.30
H-3′	3.65	3.67	3.64	3.63	3.30	3.33	3.26	3.28
H-4′	3.92	3.93	3.91	3.91	3.62	3.65	3.62	3.61
H-5′	3.72	3.75	3.61	3.69	3.30	3.48	3.28	3.31
H-$6'_R$	3.78	3.80	3.78	3.77	3.52	3.52	3.53	3.52
H-$6'_S$	3.75	3.79	3.73	3.73	3.46	3.50	3.41	3.46

[a] In D_2O. [b] In Me_2SO-d_6.

Table 4
^{13}C NMR chemical shifts (δ, ppm) for compounds **1** and **4–6** in D_2O and Me_2SO-d_6 solutions at 37°C

Carbon	Compound							
	1 [a]	**4** [a]	**5** [a]	**6** [a]	**1** [b]	**4** [b]	**5** [b]	**6** [b]
Glucose residue								
C-1	104.3	104.2	106.0	102.4	105.5	105.1	107.3	103.4
C-2	74.1	70.5	76.0	71.4	75.1	71.1	75.1	72.3
C-3	75.8	57.5	44.7	72.1	76.7	58.9	43.6	74.6
C-4	79.9	73.4	79.5	77.5	82.5	76.0	80.5	78.5
C-5	76.1	76.4	80.0	74.0	76.8	77.5	78.9	75.4
C-6	61.4	60.4	62.1	62.2	62.3	61.2	62.0	62.4
Galactose residue								
C-1′	104.4	103.3	103.5	105.5	105.7	104.9	104.8	106.5
C-2′	72.3	71.8	72.7	72.3	72.4	72.5	72.9	72.8
C-3′	73.9	73.2	74.1	74.0	75.0	75.2	75.5	75.4
C-4′	69.9	69.6	69.9	70.0	70.0	70.3	69.9	70.0
C-5′	76.7	76.6	76.6	76.5	77.4	77.9	77.0	77.1
C-6′	62.3	62.2	62.3	62.4	62.4	62.4	62.2	62.7
O-CH_3	58.4	58.5	58.5	58.5	58.0	57.9	57.8	57.8

[a] In D_2O. [b] In Me_2SO-d_6.

a ca. 60:40 (±5) distribution of *gg* and *gt* rotamers, while those for the galactose moieties do not vary with respect to **1**, and agree with combinations of the *gt* and *tg* rotamers, with the *gt* family populated [21] to the extent of ⩾65%. As previously observed for other analogues, the distribution of rotamers is basically the same in both solvents, indicating that the polarity of water and methyl sulfoxide precludes the existence of *tg* and *gg* rotamers for glucose and galactose, respectively. These rotamers could be stabilized by an intramolecular hydrogen bond between O-4 and O-6, as observed in molecular dynamics simulations in vacuo [22].

Analysis of NOE data.—An important problem for the conformational analysis of disaccharides is that of strong overlap among nuclei with potential interresidue NOE. In the case of **4–6**, H-4 does not overlap with H-3, but does overlap with H-3′ in compound **5** in dimethyl sulfoxide solution; in addition, H-1 and H-1′ appear at the same chemical shift for **4** in D_2O. Therefore, the observed presence of NOE between the anomeric protons and H-3 in steady-state and ROESY experiments does not allow us unambiguosly to neglect dipolar relaxation between H-1′ and H-3 as observed in other equatorial linked β-(1 → 4) disaccharides. These problems may be resolved through the use of modern NMR techniques. In some cases, 2D-HSMQC-ROESY experiments [23] can be employed to detect NOEs using the carbon frequencies to remove the proton frequency degeneracy. An example of the experiment for **5** is given in Fig. 3. The presence of H-1′/C-4, H-1′/C-5′, and H-1′/C-3′ connectivities can be noted as well as the intraresidue H-1/C-3 and H-1/C-5 for the glucose ring. For **4**, there is an additional problem, since C-1 and C-1′ frequencies are also very similar. In this case, the independent

Table 5
^{1}H NMR vicinal coupling constants (J, Hz) for the lateral chains of the glucose and galactose residues of compounds **1** and **4–6** in D_2O and Me_2SO-d_6 solutions at 37°C, and estimated populations of the different rotamers *gg*, *gt*, and *tg*

$^3J_{H,H}$	Compound							
	1 [a]	**4** [a]	**5** [a]	**6** [a]	**1** [b]	**4** [b]	**5** [b]	**6** [b]
Glucose residue								
D_2O								
$J_{5,6S}$	2.3	2.3	2.3	1.6	2.1	2.3	2.0	1.6
$J_{5,6R}$	5.2	5.1	5.3	5.0	3.7	5.2	5.0	4.7
%*gg*	60	60	60	65	70	60	60	65
%*gt*	40	40	40	35	30	40	40	35
Me_2SO-d_6								
$J_{5,6S}$	2.2	2.4	2.2	2.0	2.1	2.2	2.1	1.7
$J_{5,6R}$	5.1	5.5	5.2	5.3	4.6	4.6	4.4	4.5
%*gg*	60	55	60	60	65	65	65	65
%*gt*	40	45	40	40	35	35	35	35
Galactose residue								
D_2O								
$J_{5',6'S}$	4.0	3.6	4.5	4.0	4.4	3.9	4.5	4.6
$J_{5',6'R}$	8.2	7.8	7.6	8.5	7.9	7.7	6.5	8.1
%*tg*	30	35	35	30	35	10	30	35
%*gt*	70	55 [a]	65	70	65	75 [a]	50 [a]	65
Me_2SO-d_6								
$J_{5',6'S}$	4.0	5.1	6.0			4.6		4.5
$J_{5',6'R}$	8.2	7.9	7.5			7.7		7.5
%*tg*	30	35	45			35		35
%*gt*	70	65	55			65		65

[a] There is a participation of the *gg* rotamer.

cross-relaxation partners for H-1 and H-1′ could be detected using homonuclear 3D-NOESY-TOCSY experiments [24], and looking through the planes at $\omega 3 = \delta$ H-2, $\omega 3 = \delta$ H-3 to show the NOEs for the protons in the glucose ring, and, most importantly, the plane at $\omega 3 = \delta$ H-2′ or $\omega 3 = \delta$ H-3′ to detect the contacts for H-1′ and the other protons on the galactose moiety. Some of these planes are shown in Fig. 4. From the experimental data, it can be concluded that no important cross-relaxation between H-1′ and H-3 does exist for **4** and **5**. Besides, the presence of NOE between H-1′ and H-4 and not between H-2′ and H-4 implies that **4** and **5** spend most of the time in the low energy region defined by local minima **A–C**. The differentiation among these minima is more difficult since their expected interresidue contacts are very similar. Nevertheless, the presence of an NOE between H-1′ and the H-6 protons indicates that the region defined by conformer **A** is populated to some extent. An estimation of interresidue distances may be obtained by use of the isolated spin-pair approximation (ISPA), using the volumes of the cross-peaks between proton pairs in NOESY or ROESY spectra acquired with a relatively short mixing time (Table 6). This approximation leads to H-1′–H-4 distances in the range 2.2–2.5 Å, as expected for the low energy region,

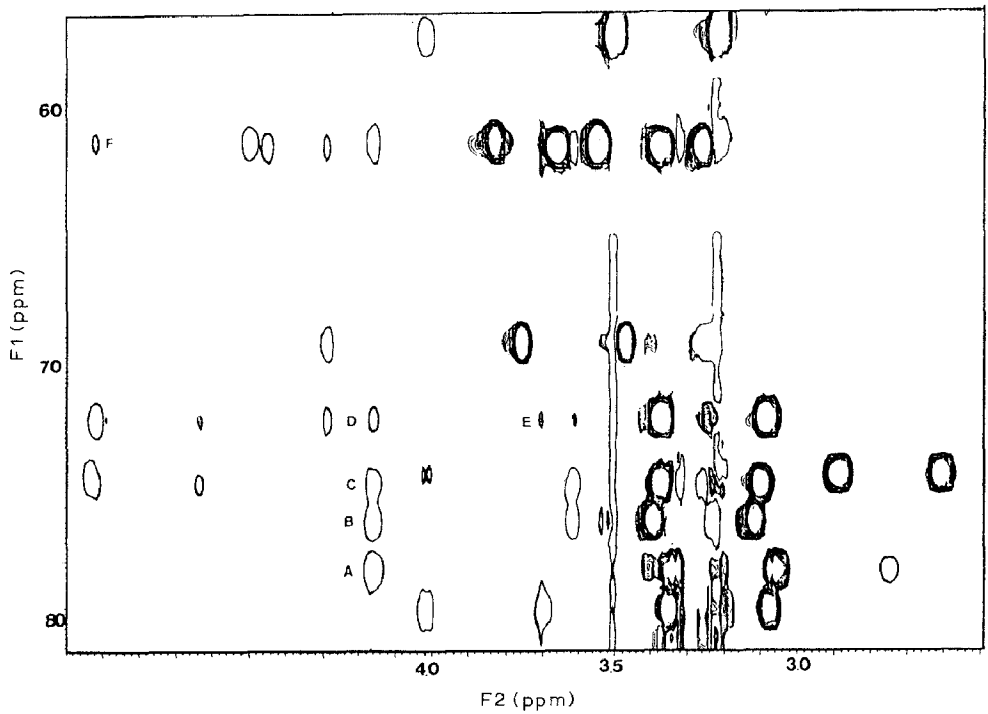

Fig. 3. HSMQC-ROESY spectrum of compound **5** in Me_2SO-d_6 at 37°C. Relevant cross-peaks are indicated A, H-1′–C-4; B, H-1′–C-5′; C, H-1′–C-3′; D, H-1′–C-2′; E, H-6–C-2′; F, HO-2′–C-6. No connectivity between H-1′ and H-3 or H-5 was detected.

without the possibility of discrimination among the different conformers. The corresponding average distance for **1** from MD simulations is 2.49 Å, although oscillations between 2.1 and 2.8 Å could be observed. The ISPA approximation leads to average H-1′–H-6 distances ranking between 3.0 and 3.5 Å, which also correspond to the low energy region. The evaluation of the expected NOEs [25–29] via a complete relaxation matrix approach [25–29] using conformers **A**–**E** allowed us to reach the same conclusion. The observed results are gathered in Tables 7 and 8. Previously, the correlation times for **2**–**4** were estimated from ^{13}C NMR T_1 measurements in both solvents at two different temperatures (Table 9). As previously observed for other oligosaccharides, a satisfactory match between the calculated and experimental intensities of H-1′–H-3′ and H-1′–H-5′ NOEs was obtained by using average correlation times ca. 30–40% higher than those estimated from the ^{13}C NMR relaxation data. The discrepancy could be due to the presence of anisotropic overall motion or to the existence of internal motions around the glycosidic linkages [30]. In fact, the observed relaxation times for C-4′ were 10–15% smaller than those for the rest of the methine carbons, indicating a slight anisotropy of the overall motion. Besides, the relaxation times for C-6 and C-6′ showed that the internal motion around both lateral chains is rather different, the one for the glucose moiety being more hindered. The comparison among the

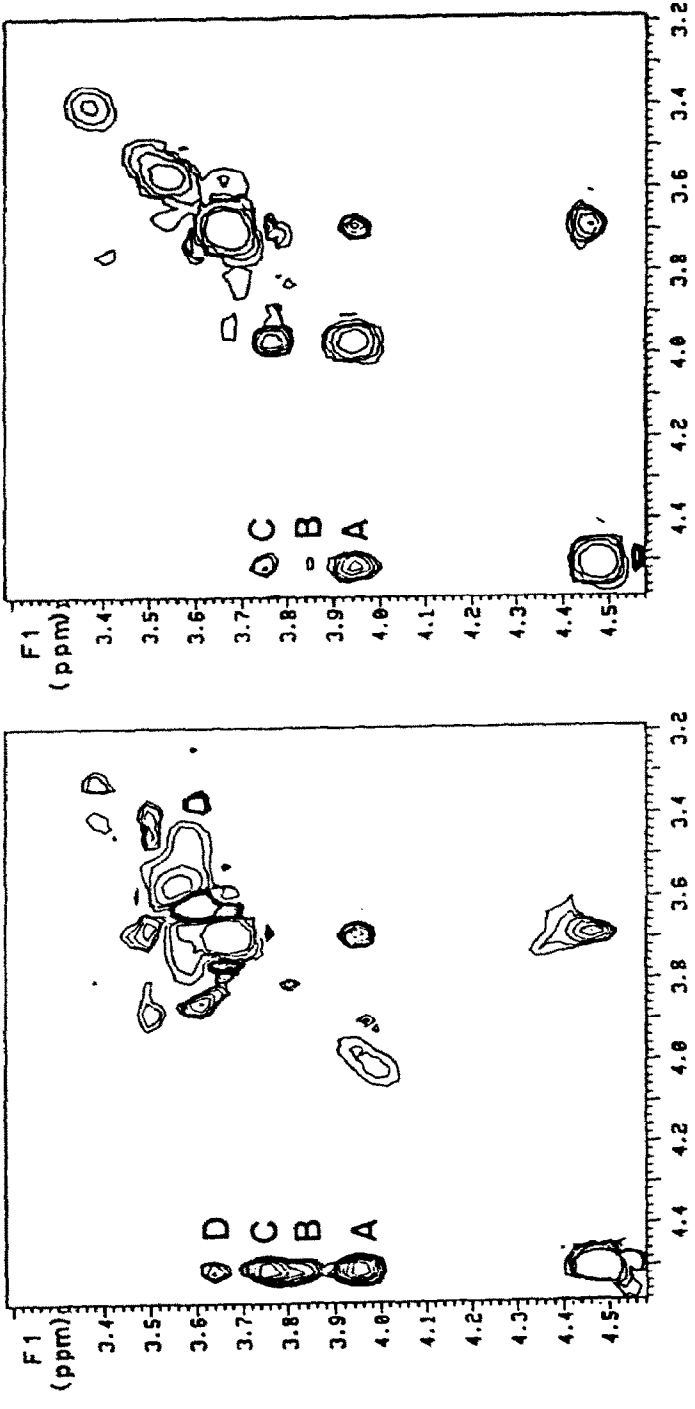

Fig. 4. Relevant 3D-NOESY-TOCSY planes of compound **4** in D_2O at 37°C. At the left-hand side, plane at F3 = δ H-2′. At the right-hand side, plane at F3 = δ *H-3′*. Relevant cross-peaks are indicated A, H-1′–*H-4*; B, H-1′–*H-6*; C, *H-1′*–*H-5′*; D, H-1′–H-3′. No connectivity between H-1′ and H-3 or H-5 was detected.

Table 6
Experimental ROESY intensities (mixing time = 0.3 s) for compounds **4**–**6** at 37°C in D_2O and at 60°C in Me_2SO-d_6 solution

Compound	Cross-peak intensity (%)							
	H-1′/3′	H-1′/5′	H-1′/4	H-1′/3	H-4′/5′	H-3′/5′	H-1/5	H-1/3
D_2O								
4	7 [a]	7 [a]	6		9 [b]	9	4	3
5	7 [a]	7 [a]	6		9 [b]	9	4	3
6	7 [a]	7 [a]	6	1	9 [b]	9	4	3
Me_2SO-d_6								
4	6 [a]	6 [a]	5		8 [b]	8	3	3
5	6 [a]	6 [a]	5		8 [b]	8	3	3
6	6 [a]	6 [a]	5		8 [b]	8	3	3

[a,b] Overlapping signals.

Table 7
Experimental and calculated [a] steady-state NOEs for compounds **4**–**6** at 37°C in D_2O solution (irradiating H-1′)

Compound	Observed NOE for signal (%)									
	H-2′	H-3′	H-4′	H-5′	H-4	H-6$_R$	H-6$_S$	H-3	H-5	CH_3
2	5	8	−1 [b]	9	12	ca. 1	ca. 1	0	0	
3	6	8	−2 [b]	10	14	ca. 1	ca. 1	0	0	0
4	6	9	−2 [b]	10	15	ca. 1	ca. 1	2	0	
	Calculated NOE for compound **4** (%)									
	H-2′	H-3′	H-4′	H-5′	H-4	H-6$_R$	H-6$_S$	H-3	H-5	
Conformer **A**	7	9	−2	10	18	2	−0.7			
Conformer **B**	5	8	−1	9	14					
Conformer **C**	5	8	−2	10	17					
Conformer **D**	3	10	−2	11						
Conformer **E**	7	10	−2	11				32		
	Calculated NOE for compound **5** (%)									
	H-2′	H-3′	H-4′	H-5′	H-4	H-6$_R$	H-6$_S$	H-3	H-5	CH_3
Conformer **A**	8	8	−2	9	13	4	−1			
Conformer **B**	8	8	−1	5	13					7
Conformer **C**	8	8	−2	9	16					2
Conformer **D**	3	8	−2	9						
Conformer **E**	8	8	−2	7				29	7	
	Calculated NOE for compound **6** (%)									
	H-2′	H-3′	H-4′	H-5′	H-4	H-6$_R$	H-6$_S$	H-3	H-5	
Conformer **A**	8	8	−2	9	15	2	−1	−1		
Conformer **B**	8	8	−1	8	15			7		
Conformer **C**	8	8	−2	9	15			10		
Conformer **D**	4	8	−2	9						
Conformer **E**	9	8	−2	8				4	10	

[a] Using the full-matrix relaxation method and $\tau_c = 0.10 \times 10^{-9}$ s. [b] Three-spin effect produces negative NOE.

Table 8
Experimental and calculated [a] steady-state NOEs for compounds **4–6** at 60°C in Me_2SO-d_6 solution

Compound	Observed NOE for signal (%)									
	H-2′	H-3′	H-4′	H-5′	H-4	H-6$_R$	H-6$_S$	H-3	H-5	CH_3
4	5	7	−1 [b]	8	10	0	0	0	0	
5	5	7	−1 [b]	8	11	0	0	0		0
6	5	7	−1 [b]	8	13	0	0	0		
	Calculated NOE for compound **4** (%)									
	H-2′	H-3′	H-4′	H-5′	H-4	H-6$_R$	H-6$_S$	H-3	H-5	
Conformer **A**	6	8	−1	8	16	1				
Conformer **B**	4	7	−1	9	13					
Conformer **C**	4	7	−1	8	16					
Conformer **D**	2	8	−1	9						
Conformer **E**	6	8	−1	9				25		
	Calculated NOE for compound **5** (%)									
	H-2′	H-3′	H-4′	H-5′	H-4	H-6$_R$	H-6$_S$	H-3	H-5	CH_3
Conformer **A**	7	7	−1	8	11	2				
Conformer **B**	6	6	−1	4	11					6
Conformer **C**	6	7	−1	8	14					1
Conformer **D**	2	6	−1	8						
Conformer **E**	7	7	−1	6				23	6	
	Calculated NOE for compound **6** (%)									
	H-2′	H-3′	H-4′	H-5′	H-4	H-6$_R$	H-6$_S$	H-3	H-5	
Conformer **A**	7	7	−1	8	13	1				
Conformer **B**	7	6	−1	7	13			6		
Conformer **C**	7	7	−1	8	13			8		
Conformer **D**	3	6	−1	8				7		
Conformer **E**	8	7	−1	7					8	

[a] Using the full-matrix relaxation method and $\tau_c = 0.15 \times 10^{-9}$ s. [b] Three-spin effect produces negative NOEs.

observed and calculated interresidue cross-peaks H-1′–H-4 and H-1′–H-6$_{proS,R}$ for the different individual conformers indicated that the presence of conformers **D** or **E** to an appreciable extent can be discarded since they would produce H-1′–H-4

Table 9
Experimental average methine ^{13}C NMR relaxation times (T_1, s) and corresponding average correlation times (τ_c, 10^{-9} s) for compounds **4–6** in D_2O at 37°C and Me_2SO-d_6 at 37 and 60°C

Compound	Solvent					
	D_2O		Me_2SO-d_6 (37°C)		Me_2SO-d_6 (60°C)	
	T_1	τ_c	T_1	τ_c	T_1	τ_c
4	0.70	0.08	0.45	0.13	0.61	0.09
5	0.73	0.07	0.45	0.13	0.61	0.09
6	0.73	0.07	0.43	0.13	0.63	0.09

intensities noticeably smaller than those observed along with NOEs for the H-1′–H-3 and/or H-2′–H-4 contacts that were not observed either in steady state or ROESY measurements. The data agree with the conclusion estimated from the use of the ISPA. On the other hand, the existence of a small NOE (ca. 2%) between H-1′ and H-3 for the 3-epi analogue **6** indicates that no unique conformer can explain the observed NOEs, and therefore there is a certain flexibility for the glycosidic linkage within the area described by **A**–**C** conformers. Nevertheless, these results indicate that the extent of flexibility around the β-(1 → 4) linkage in compounds **4**–**6** in water or dimethyl sulfoxide solutions is rather small, and the NMR data can be satisfactorily explained by considering contributions of conformers defined by $\Phi = 15 \pm 45°$ and $\Psi = -25 \pm 30°$. Therefore, only ca. 5% of the complete potential energy surface is populated in solution. The recognition of conformers **D** or **E** should therefore be accompanied by the formation of several hydrogen bonds or stabilizing van der Waals contacts to override the important energy barrier between the low energy region and these islands. Similar results have been reported for different equatorial β-(1 → 4)-linked oligosaccharides. Although a great area of the low energy region matches the geometrical requirements for the formation of an O-3–O-5′ hydrogen bond for **1**, the results obtained for **4**–**6** in both water and dimethyl sulfoxide indicate that the formation of this hydrogen bond is not essential for the presence of an important proportion of **A** and **B** conformers. In fact, although the existence of the corresponding hydrogen bond in methyl β-cellobioside has been recently demonstrated in Me_2SO-d_6, there are contradictory results in water solutions where it has been reported to disappear [31]. On the other hand, it has been postulated to exist in 6′-*O*-sialyl-lactose [32]. Assuming that the interaction with the lectin takes place in one of these conformations [3], the observed dissociation constants may be used to correlate structure and activity.

Binding studies.—Compounds **4**–**6** were tested as inhibitors of the binding of ricin to Sepharose 6B. The apparent dissociation constants, calculated as described in Materials and Methods, are given in Table 10. The data previously obtained [1] for the 3-deoxy (**2**) and 3-*O*-methyl (**3**) derivatives are also included for comparative purposes.

Table 10
Apparent dissociation constants for the binding of methyl β-lactoside derivatives to ricin: inhibition assays were carried out at pH 7.6

Compound	K_d (μM)
1	56 ± 5 [a]
2	27 ± 9 [a]
3	311 ± 3 [a]
4	378 ± 15
5	87 ± 3
6	390 ± 20

[a] Data taken from Rivera-Sagredo et al. [1].

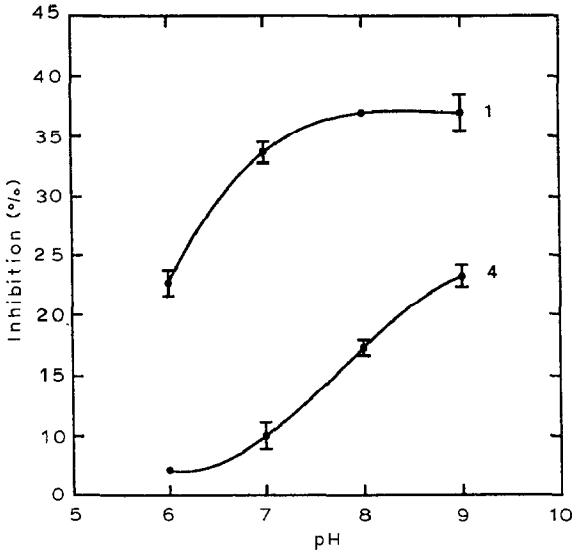

Fig. 5. pH-Dependent inhibition of ricin binding to Sepharose by methyl β-lactoside (**1**) and its 3-aminodeoxy derivative (**4**). Concentrations used were 0.2 mM for **1** and 0.4 mM for **4**.

The observed enhancement of the strength of the binding on replacement of the HO-3 group by hydrogen [1] suggested a nonpolar interaction of this part of the molecule with the protein. Intramolecular hydrogen bonding could result in this region becoming more lipophilic in character and, in fact, the preferred average conformation [1] of methyl β-lactoside (**1**) allows the formation of a hydrogen bond between HO-3 and O-5′. Therefore, it was suggested [1] that the hydroxyl group at this position is accepted into a nonpolar region near the periphery of the combining site by becoming intramolecularly bonded.

Replacement of HO-3 by an amino group, to form **4**, resulted in a weaker inhibitor. The presence of a charged group in a nonpolar environment should result in a strong destabilizing effect that could give rise to a lower affinity for **4** than for **1**. Accordingly, the inhibitor potency of the amino derivative increased with increasing pH from 7 to 9, whereas that of **1** remained rather constant (Fig. 5). In agreement with previous observations [33,34], the binding ability of ricin decreased markedly below pH 7. At pH 9, where the amino group should exist extensively as the free base, the inhibitory potency of **4** was still lower than that shown by **1**. An approximate apparent dissociation constant at this pH of 180 μM was estimated from the data shown in Fig. 5, as compared to 53 μM for **1**. The decreased activity of the amino derivative could be related to the fact that, although the conformational preferences of both compounds were very similar, no intramolecular hydrogen bond between H_2N-3 and O-5′ was observed. On the contrary, the C-3 region in **1** becomes more lipophilic in character by virtue of intramolecular hydrogen bonding of the 3-hydroxyl, thus favouring the binding.

The orientation of HO-3 which would allow such a bond seems also to be required to minimize steric hindrances upon binding. As had been previously observed [1] for the 3-*O*-methyl derivative (**3**), the affinity for the 3-epi analogue (**6**) was decreased. Besides the inability to form the above-mentioned hydrogen bond, the lower affinity exhibited for the binding of these two compounds, as compared to **4** in its free base form, could be attributed to the introduction of a steric destabilizing effect. A similar steric destabilization could account for the lower affinity of **5** as compared to the deoxy analogue in spite of the nonpolar nature of the CH_3 substituent.

As revealed by X-ray crystallographic studies [4], the two binding sites present in ricin B-chain are shallow pockets in which the top of the pocket is formed by the side chain of an aromatic residue, Trp37 in the low-affinity site and Tyr248 in the high-affinity site. The data obtained on the basis of inhibition of the binding of ricin to Sepharose relate to the high-affinity binding site [35]. Docking studies on the conformers of methyl β-melibioside bound to ricin B-chain [6] have shown that, since the galactose ring is slightly more embedded into the C-terminal site, only a small rotation about the galactose C-4 is enough to translate bad steric contacts of the glucose ring with Tyr248 into what could be favourable hydrophobic contacts. Although the spatial position of the glucose ring with respect to the galactose moiety in the β-(1 → 4) and the α-(1 → 6) linkages is different, the results here reported suggest that similar nonpolar interactions could be present in the binding of methyl β-lactoside to ricin.

3. Experimental

NMR experiments.—NMR spectra were recorded at 37°C in D_2O, and at 37 and 60°C in Me_2SO-d_6 with a Varian Unity 500 spectrometer. Proton chemical shifts were referenced to residual HDO at δ 4.64 or residual Me_2SO-d_5 at δ 2.49. Carbon chemical shifts were referenced to external dioxane at δ 67.4 ppm.

The 1D-NOE, DQF-COSY, TOCSY, CAMELSPIN (ROESY), HMQC, and HSMQC-ROESY experiments and the ^{13}C NMR T_1 measurements were performed in the phase-sensitive mode as previously described [23].

The 3D-NOESY-TOCSY experiment was performed using the pulse sequence described by Vuister et al. [24], although quadrature detection along F1 and F2 was achieved following the method of States et al. [36]; 128 independent increments of 1K complex points (eight scans each) were acquired for both evolution periods. One level of zero-filling was used before Fourier transformation with Varian software.

Molecular mechanics and dynamics calculations.—The MM2 low-energy conformers found previously [1] for **1** (**A**, **B**, **C**/**C′**, **D**, **E**) were modified at the desired position and submitted to further energy minimization. Torsion angles at the glycosidic linkages are defined as Φ H-1′–C-1′–O-1′–C-4 and Ψ C-1′–O-1′–C-4–H-4. Only the *gt* conformation of the lateral chain was used for the galactose residue, while both the *gg* and *gt* rotamers were considered for the glucose moiety

[16]. In all cases, both Φ and Ψ angles showed slight variations (ca. $\pm 15°$) from the starting point. A dielectric constant of 1.5 D was used. The geometries of **1** describing minima A, D, and E (*gg* for the glucose residue) were then taken as starting structures for MD calculations in vacuo by using the CVFF [37] and the AMBER [38] force field as integrated in the Discover 2.8 program. The MD simulations were performed at 303 K with a dielectric constant of 78 D and a time step of 1 fs. The equilibration time was 20 ps and the total simulation time was 1 ns. Trajectory frames were saved every 0.5 ps. The trajectories were examined with the Analysis module of INSIGHT II [39].

The steady-state 1D-NOE experiments were calculated according to the complete relaxation matrix method by using the NOEMOL program [26] for the geometries of conformers **A**–**E**. Isotropic motion and no external relaxation were assumed in the calculation process. Different τ_c values were tested in order to get the best match between the experimental and the calculated NOE for a given intraresidue proton pair. ROESY (CAMELSPIN) experiments were used to estimate interproton distances according to the isolated spin-pair approximation (ISPA) [22].

Binding studies: materials and methods.—Ricin was obtained from *Ricinus communis* seeds (Jardín Botánico, C.S.I.C., Madrid, Spain) as previously reported [40]. The lectin was separated from *Ricinus communis* agglutinin by gel filtration on Sephadex G-100 and enzymatically labelled with ^{125}I in the presence of 0.1 M lactose, using Iodogen as instructed by the manufacturer. ^{125}I-ricin was indistinguishable from the unlabelled protein as determined by SDS-polyacrylamide gel electrophoresis and autoradiography. The concentration of the lectin was estimated spectrophotometrically using a value of $A^{1\%}_{280} = 14$ (ref. [41]).

The affinity of the ricin for the sugar derivatives was estimated by determining the amount of ^{125}I-ricin bound to Sepharose 6B in the presence of different concentrations of the sugar as described previously [1,2]. The standard assay was carried out in 5 mM phosphate buffer, pH 7.6, containing 0.2 M NaCl. More than 70% of ricin was bound to Sepharose in the absence of sugar and less than 3% of the radioactivity applied was trapped on the gel in the presence of 0.1 M lactose (final concentration).

Methyl β-lactoside derivatives were first tested in a "range-finding" experiment using inhibitor concentrations from 40 μM to 2 mM. For determination of the apparent dissociation constants, inhibition was assayed afterwards at the range of concentrations of each derivative producing from 10 to 65% inhibition of the binding of ricin to Sepharose. The K_d values were calculated from the plot of the reciprocal of the lectin fraction bound to Sepharose versus the inhibitor concentration, as previously described [1,2].

Inhibition assays at various pH values were carried out in a citrate–phosphate (pH 6.0–7.0), phosphate (pH 7.0–8.0), or carbonate–phosphate (pH 8.0–9.0) buffer (5 mM), all of them containing 0.2 M NaCl.

General procedures.—Melting points were determined on a Kofler hot-stage apparatus and are uncorrected. TLC was performed on Silica Gel GF_{254} (Merck) with detection by charring with H_2SO_4. Column chromatography was performed

on silica gel (70–230 mesh, Merck). Spectral data were recorded on the following instruments: IR, Perkin–Elmer 681 spectrophotometer; optical rotations, Perkin–Elmer 241 MC polarimeter; NMR, Varian XL-300, Varian Unity 500, and Bruker AM-200 spectrometers.

Materials.—Methyl 2,6,2',3',4',6'-hexa-O-benzyl-β-lactosid-3-ulose (**8**). A solution of Me_2SO (3.3 equiv, 182 mL) in CH_2Cl_2 (0.6 mL) was added to a solution of oxalyl chloride (1.5 equiv, 102 mL) in CH_2Cl_2 (2.5 mL) at −45°C under Ar during 5 min. After stirring for 20 min, a solution of **7** (0.6 g, 0.668 mmol) in CH_2Cl_2 (1 mL) was added during 5 min, and left for 15 min more. Then, *N*-ethyldiisopropylamine (6.7 equiv, 907 mL) was added during 5 min, and the mixture was allowed to attain room temperature. After addition of water (2.5 mL) and stirring for 10 min, the phases were separated, and the aqueous phase was extracted with CH_2Cl_2. The combined organic phases were washed with 0.5 M HCl, satd aq $NaHCO_3$ and water, dried over $NaSO_4$, and concentrated. Column chromatography (4 : 1 hexane–EtOAc) of the residue gave **8** (0.4 g, 67%) as a syrup; $[\alpha]_D^{20}$ −1.5° (*c* 2.1, $CHCl_3$); NMR data ($CDCl_3$): ^{13}C (50 MHz), δ 200.0 (C=O); IR (NaCl): ν_{max} 1740 (m) cm^{-1}. Anal. Calcd for $C_{55}H_{58}O_{11}$: C, 73.81; H, 6.53. Found: C, 73.68; H, 6.64.

Methyl 3-amino-2,6,2',3',4',6'-hexa-O-benzyl-3-deoxy-β-lactoside (**10**).—A mixture of **8** (0.219 g, 0.245 mmol), benzoxyamine hydrochloride (2.7 equiv, 0.111 g), and pyridine (11 mL) was heated at 60°C for 2 h. Pyridine was removed under reduced pressure and the residue was purified by chromatography (4 : 1 hexane–EtOAc) to yield a (*Z*,*E*)-mixture of **9** (0.205 g, 84%) as an oil; IR (NaCl): no CO absorption.

The *O*-benzyloximes **9** (0.205 g, 0.21 mmol) dissolved in diethyl ether (1.5 mL) were added under Ar at 0° to an ethereal solution (5 mL) of $LiAlH_4$ (1.6 equiv, 12 mg). The mixture was stirred for 4 h at room temperature, quenched with satd aq NH_4Cl, and left overnight. The organic phase was extracted with EtOAc. After removal of the solvent, the crude product was chromatographed (2 : 1 hexane–EtOAc) to give methyl 3-amino-2,6,2',3',4',6'-hexa-*O*-benzyl-3-deoxy-3-*epi*-β-lactoside (**11**; 51 mg, 25%); and **10** (87 mg, 43%) as an oil; $[\alpha]_D^{20}$ +8° (*c* 1.2, $CHCl_3$); NMR data ($CDCl_3$): ^1H (300 MHz), δ 7.32–7.18 (m, 30 H, Ph), 4.92 and 4.55 (ABq, 2 H, *J* 11.5 Hz, CH_2Ph), 4.88 and 4.61 (ABq, 2 H, *J* 11.8 Hz, CH_2Ph), 4.79 and 4.72 (ABq, 2 H, *J* 11.2 Hz, CH_2Ph), 4.66 (s, 2 H, CH_2Ph), 4.42 and 4.28 (ABq, 2 H, *J* 12.1 Hz, CH_2Ph), 4.38 (s, 2 H, CH_2Ph), 4.28 (d, 1 H, $J_{1',2'}$ 7.6 Hz, H-1'), 4.26 (d, 1 H, $J_{1,2}$ 7.7 Hz, H-1), 3.88 (bd, 1 H, $J_{3',4'}$ 2.6 Hz, H-4'), 3.71 (dd, 1 H, H-6a), 3.69 (t, 1 H, $J_{3,4} = J_{4,5} = 9.2$ Hz, H-4), 3.58 (dd, 1 H, H-6b), 3.57 (d, 1 H, H-6'a), 3.51 (m, 1 H, H-6'b), 3.51 (s, 3 H, OCH_3), 3.47–3.41 (m, 3 H, H-5,2',5'), 3.37 (dd, 1 H, $J_{2',3'}$ 9.8, $J_{3',4'}$ 2.9 Hz, H-3'), 3.17 (dd, 1 H, $J_{1,2}$ 7.7, $J_{2,3}$ 9.7 Hz, H-2), 2.95 (t, 1 H, $J_{3,4} = J_{4,5} = 9.2$ Hz, H-3), 1.78 (bs, 1 H, OH); ^{13}C (50 MHz), δ 138.7, 138.5, 138.4, 138.2, 137.7 (6 C-ipso, Ph), 128.3–127.2 (Ph), 104.6, 103.5 (C-1,1'), 82.4, 82.3, 79.3, 79.1, 75.9, 73.2, 72.7 (C-2,4,5 and C-2'–5'), 75.2, 74.7, 74.5, 73.3, 72.9, 72.7 (6 CH_2Ph), 68.4, 67.9 (C-6,6'), 56.8, 56.5 (OCH_3, C-3). Anal. Calcd for $C_{55}H_{61}NO_{10}$: C, 73.72; H, 6.86; N, 1.56. Found: C, 73.47; H, 7.07; N, 1.69.

Methyl 3-amino-3-deoxy-β-lactoside (**4**).—A solution of **10** (70 mg, 0.08 mmol) in

1:1 CH_2Cl_2–EtOH (14 mL) was hydrogenated in the presence of 10% Pd–C (70 mg) for 15 h at atmospheric pressure. The catalyst was removed by filtration through Celite, and the solvents were evaporated. Column chromatography of the residue (4:1 $CHCl_3$–MeOH) gave **4** (26 mg, 94%) as a white solid; mp 149–151°C; $[\alpha]_D^{20}$ −2.7° (*c* 0.7, H_2O); NMR data (D_2O): ^1H (500 MHz), δ 4.48 (d, 1 H, $J_{1,2}$ 7.5 Hz, H-1), 4.48 (d, 1 H, $J_{1',2'}$ 7.5 Hz, H-1'), 3.99 (dd, 1 H, $J_{5,6a}$ 2.2, $J_{6a,6b}$ 12.3 Hz, H-6a), 3.95 (t, 1 H, $J_{3,4} = J_{4,5} = 9.8$ Hz, H-4), 3.93 (bd, 1 H, $J_{3',4'}$ 3.1 Hz, H-4'), 3.83 (dd, 1 H, $J_{5,6b}$ 5.0, $J_{6a,6b}$ 12.5 Hz, H-6b), 3.80 (m, 1 H, H-6'a), 3.79 (m, 1 H, H-6'b), 3.75 (ddd, 1 H, $J_{5',6'a}$ 5.0, $J_{6'a,6'b}$ 12.0 Hz, H-5'), 3.71 (ddd, 1 H, $J_{5,6a}$ 2.3 Hz, H-6a), 3.67 (dd, 1 H, $J_{2',3'}$ 10.0, $J_{3',4'}$ 3.5 Hz, H-3'), 3.59 (s, 3 H, OCH_3), 3.56 (dd, 1 H, $J_{1',2'}$ 8.0, $J_{2',3'}$ 10.0 Hz, H-2'), 3.51 (dd, 1 H, $J_{1,2}$ 7.5, $J_{2,3}$ 10.5 Hz, H-2), 3.38 (t, 1 H, $J_{2,3} = J_{3,4} = 10.3$ Hz, H-3); ^{13}C (125 MHz), δ 104.2 (C-1), 103.3 (C-1'), 76.6 (C-5'), 76.4 (C-5), 73.4 (C-4), 73.2 (C-3'), 71.8 (C-2'), 70.5 (C-2), 69.6 (C-4'), 62.2 (C-6'), 60.4 (C-6), 58.5 (OCH_3), 57.5 (C-3). Anal. Calcd for $C_{55}H_{61}NO_{10}$: C, 73.72; H, 6.86; N, 1.56. Found: C, 73.47; H, 7.07; N, 1.69.

Methyl 2,6,2',3',4',6'-hexa-O-benzyl-3-deoxy-3-C-methylene-β-lactoside (**12**).—A solution of butyllithium in hexane (1.3 equiv, 0.74 mL) was added at room temperature to a stirred suspension of finely ground methyltriphenylphosphonium bromide (1.5 equiv, 0.191 g) in dry ether (3.3 mL) under N_2. After stirring for 1.5 h, a solution of the ketone **8** (0.320 g, 0.36 mmol) in toluene (6 mL) was added and the mixture was stirred for 16 h. Water (4 mL) was added and, after stirring for 6 h, the phases were separated. The aqueous phase was extracted with CH_2Cl_2 and ether, and the combined organic phases were dried and concentrated. Column chromatography (5:1 hexane–EtOAc) of the residue gave **12** (0.131 g, 37%; 51% on starting material recovered) as an oil; $[\alpha]_D^{20}$ +7.6° (*c* 0.8, $CHCl_3$); NMR data ($CDCl_3$): ^1H (300 MHz), δ 5.52 (d, 1 H, J_{gem} 2.0 Hz, C=CH_2), 5.37 (d, 1 H, J_{gem} 2.0 Hz, C=CH_2); ^{13}C, δ 109.6 (C=$\underline{C}H_2$). Anal. Calcd for $C_{56}H_{60}O_{10}$: C, 75.31; H, 6.77. Found: C, 75.02; H, 6.77.

Methyl 3-deoxy-3-C-methyl-β-lactoside (**5**).—Pd–C (10%, 30 mg) was added to a solution of **12** (0.119 g, 0.13 mmol) in 1:1 CH_2Cl_2–EtOH (10 mL) at atmospheric pressure. The mixture was processed as described above, to obtain 46 mg (98%) of a mixture of epimers at C-3. The mixture was benzoylated under conventional conditions and crystallized from MeOH to yield methyl 2,6,2',3',4',6'-hexa-*O*-benzoyl-3-deoxy-3-*C*-methyl-β-lactoside (**13**) as a white solid; mp 128–130°C; $[\alpha]_D^{20}$ +68° (*c* 0.8, $CHCl_3$); NMR data ($CDCl_3$): ^1H (200 MHz), δ 8.14–7.19 (m, 30 H, Ph), 5.94 (d, 1 H, $J_{3',4'}$ 3.3 Hz, H-4'), 5.84 (dd, 1 H, $J_{1',2'}$ 7.8, $J_{2',3'}$ 10.4 Hz, H-2'), 5.50 (dd, 1 H, $J_{3',4'}$ 3.4, $J_{2',3'}$ 10.4 Hz, H-3'), 4.97–4.88 (m, 2 H), 4.54–4.41 (m, 4 H), 4.43 (d, 1 H, $J_{1',2'}$ 7.8 Hz, H-1'), 4.17 (m, 1 H, H-5 or 5'), 3.77 (t, 1 H, $J_{3,4} = J_{4,5} = 9.6$ Hz, H-4), 3.70 (m, 1 H, H-5 or 5'), 3.38 (s, 3 H, OCH_3), 2.30 (m, 1 H, H-3), 1.23 (d, 3 H, $J_{H\text{-}3,CH_3}$ 6.4 Hz, CH_3); ^{13}C (50 MHz), δ 166.0, 165.9, 165.4, 165.0 (6 C=O), 133.6, 133.4, 133.3 (6 C-ipso, Ph), 130.1–128.3 (Ph), 103.1, 100.6 (C-1/1'), 77.4, 75.6, 73.9, 71.8, 71.5, 69.9, 68.0 (C-2,4,5 and C-2'–5'), 63.0, 62.0 (C-6/6'), 55.6 (OCH_3) 40.2 (C-3), 14.5 (CH_3). Anal. Calcd for $C_{56}H_{50}O_{11}$: C, 68.70; H, 5.15. Found: C, 68.45; H, 5.40.

Zemplén deacylation of **13** gave **5** as a white solid; mp 134–136°C; $[\alpha]_D^{20}$ −3.8°

(*c* 0.23, H_2O); NMR data (D_2O): ^1H (500 MHz), δ 4.41 (d, 1 H, $J_{1',2'}$ 7.8 Hz, H-1'), 4.36 (d, 1 H, $J_{1,2}$ 7.9 Hz, H-1), 4.03 (dd, 1 H, $J_{5,6a}$ 2.2, $J_{6a,6b}$ 12.1 Hz, H-6a), 3.91 (bd, 1 H, $J_{3',4'}$ 3.5 Hz, H-4'), 3.78 (dd, 1 H, $J_{5',6'a}$ 5.6, $J_{6'a,6'b}$ 12.1 Hz, H-6'a), 3.76 (m, 1 H, H-6b), 3.73 (d, 1 H, $J_{5',6'b}$ 2.8 Hz, H-6'b), 3.64 (dd, 1 H, $J_{2',3'}$ 9.8, $J_{3',4'}$ 3.5 Hz, H-3'), 3.61 (m, 1 H, H-5'), 3.60 (m, 1 H, H-5), 3.54 (s, 3 H, OCH_3), 3.51 (dd, 1 H, $J_{1',2'}$ 7.7 Hz, H-2'), 3.50 (t, 1 H, $J_{3,4} = J_{4,5} = 10.0$ Hz, H-4), 3.08 (dd, 1 H, $J_{1,2}$ 7.9, $J_{2,3}$ 10.6 Hz, H-2), 1.72 (ddq, 1 H, J_{H,CH_3} 6.4, $J_{2,3} = J_{3,4} = 10.3$ Hz, H-3), 1.18 (s, 3 H, $J_{H\text{-}3,CH_3}$ 6.4 Hz, CH_3); ^{13}C (125 MHz), δ 160.0 (C-1), 103.5 (C-1'), 80.0 (C-5), 79.5 (C-4), 76.6 (C-5'), 76.0 (C-2), 74.1 (C-3'), 72.7 (C-2'), 69.9 (C-4'), 62.3 (C-6'), 62.1 (C-6), 58.5 (OCH_3), 44.7 (C-3). Anal. Calcd for $C_{55}H_{61}NO_{10}$: C, 73.72; H, 6.86; N, 1.56. Found: C, 73.47; H, 7.07; N, 1.69.

*Methyl 3-*O*-acetyl-2,6,2',3',4',6'-hexa-*O*-benzyl-3-*epi*-β-lactoside* (**14**).—Trifluoromethanesulfonic anhydride (3 equiv, 16 mL) was slowly added to a solution of **7** (0.28 g, 0.31 mmol) and pyridine (6 equiv, 15 mL) in CH_2Cl_2 (10 mL), at −20°C under Ar. The solution was stirred at room temperature for 1.5 h, diluted with CH_2Cl_2, and poured onto ice–$NaHCO_3$. The organic layer was subsequently washed with 10% HCl, water, and satd aq $NaHCO_3$, and dried ($NaSO_4$), and the solvent evaporated. A solution of the resulting crude triflate and tetrabutylammonium acetate (11 equiv, 1.04 g) in toluene (6 mL) was kept overnight at room temperature under Ar. Concentration to dryness, followed by chromatography (5 : 1 hexane–EtOAc) gave **14** (0.198 g, 76.5%) as an oil; $[\alpha]_D^{20}$ −6.9° (*c* 0.8, $CHCl_3$); NMR data ($CDCl_3$): ^1H (300 MHz), δ 7.35–7.20 (m, 30 H, 6 Ph), 5.85 (t, 1 H, $J_{2,3} = J_{3,4} = 2.9$ Hz, H-3), 4.91 and 4.69 (ABq, 2 H, *J* 11.7 Hz, CH_2Ph), 4.78 and 4.72 (ABq, 2 H, *J* 11.0 Hz, CH_2Ph), 4.75 (d, 1 H, $J_{1,2}$ 8.3 Hz, H-1), 4.68 (s, 2 H, CH_2Ph), 4.64 and 4.55 (ABq, 2 H, *J* 11.7 Hz, CH_2Ph), 4.49 and 4.39 (ABq, 2 H, *J* 11.9 Hz, CH_2Ph), 4.44 (d, 2 H, CH_2Ph), 4.37 (d, 1 H, $J_{1',2'}$ 7.7 Hz, H-1'), 3.96 (ddd, 1 H, $J_{4,5}$ 9.9, $J_{5,6a}$ 5.3, $J_{5,6b}$ 1.4 Hz, H-5), 3.88 (bd, 1 H, $J_{3',4'}$ 2.8 Hz, H-4'), 3.75 (dd, 1 H, $J_{3,4}$ 2.6, $J_{4,5}$ 9.8 Hz, H-4), 3.78–3.55 (m, 5 H, 6a,6b,5',6'a,6'b), 3.53 (s, 3 H, OCH_3), 3.46–3.40 (m, 2 H, H-2',3'), 3.29 (dd, 1 H, $J_{1,2}$ 7.8, $J_{2,3}$ 3.0 Hz, H-2), 2.20 (s, 3 H, Ac); ^{13}C (50 MHz), δ 169.5 (C=O), 138.9, 138.7, 138.4, 138.1, 138.0 (6 C-ipso, Ph), 128.4–127.4 (Ph), 103.4, 101.2 (C-1,1'), 82.3, 79.3, 76.5, 73.5, 73.4, 73.0, 69.8 (C-2–5 and C-2'–5'), 75.1, 74.5, 73.2, 72.6, 71.9 (6 CH_2Ph), 69.1, 68.4 (C-6,6'), 56.8 (OCH_3), 21.1 (Ac).

*Methyl 3-*epi*-β-lactoside* (**6**).—Conventional hydrogenolysis of **14** as described above, followed by filtration through Celite and concentration, gave a residue which was treated with methanolic NaOMe for 2 h. The solution was neutralized with Amberlite IR-120 (H^+), filtered, and evaporated. Column chromatography (4 : 1 CH_2Cl_2–MeOH) afforded **6** (65 mg, 89%) as a white solid; NMR data (D_2O): ^1H (500 MHz), δ 4.63 (d, 1 H, $J_{1,2}$ 8.0 Hz, H-1), 4.49 (d, 1 H, $J_{1',2'}$ 7.5 Hz, H-1'), 4.42 (t, 1 H, $J_{2,3} = J_{3,4} = 3.0$ Hz, H-3), 3.96 (dd, 1 H, $J_{5,6a}$ 2.3, $J_{6a,6b}$ 12.3 Hz, H-6a), 3.92 (bd, 1 H, $J_{3',4'}$ 3.5 Hz, H-4'), 3.88 (dd, 1 H, $J_{4,5}$ 10.0, $J_{5,6a}$ 5.5, $J_{5,6b}$ 2.0 Hz, H-5), 3.79 (dd, 1 H, H-4), 3.78–3.73 (m, 3 H, H-6b,6'a,6'b), 3.66 (m, 1 H, H-5'), 3.64 (dd, 1 H, $J_{2',3'}$ 10.3, $J_{3',4'}$ 3.5 Hz, H-3'), 3.56 (s, 3 H, OCH_3), 3.55 (dd, 1 H, $J_{1',2'}$ 7.8, $J_{2',3'}$ 9.8 Hz, H-2'), 3.46 (dd, 1 H, $J_{1,2}$ 8.5, $J_{2,3}$ 3.0 Hz, H-2); ^{13}C (125 MHz), δ 105.5 (C-1'), 102.4 (C-1), 77.5 (C-4), 76.5 (C-5'), 74.0 (C-5,3'), 72.3 (C-2'),

71.4 (C-2), 70.0 (C-4′), 62.4 (C-6′), 62.2 (C-6), 58.5 (OCH_3). Anal. Calcd for $C_{55}H_{61}NO_{10}$: C, 73.72; H, 6.86; N, 1.56. Found: C, 73.47; H, 7.07; N, 1.69.

4. Acknowledgments

We thank Professor M. Bernabé and Dr. A. Rivera (Madrid) for helpful discussions, Dr. M. Forster (Potters Bar, UK) for the use of the NOEMOL programme, and Dr. A. Imberty (Nantes, France) for a preprint of ref 12 prior to publication. Fundings from DGICYT (project PB-87-367) and CICYT (project SAF 92/0497) are gratefully acknowledged.

5. References

[1] A. Rivera-Sagredo, D. Solis, T. Diaz-Mauriño, J. Jiménez-Barbero, and M. Martín-Lomas, *Eur. J. Biochem.*, 197 (1991) 217–228.
[2] A. Rivera-Sagredo, D. Solis, T. Diaz-Mauriño, J. Jiménez-Barbero, and M. Martín-Lomas, *Carbohydr. Res.*, 232 (1992) 207–226.
[3] V.L. Bevilacqua, D.S. Thomson, and J.H. Prestegard, *Biochemistry*, 29 (1990) 5529–5537.
[4] E. Rutenber and J.D. Robertus, *Proteins*, 10 (1991) 260–269.
[5] J.U. Baenziger and D. Fiete, *J. Biol. Chem.*, 254 (1979) 9795–9799.
[6] V.L. Bevilacqua, Y. Kim, and J.H. Prestegard, *Biochemistry*, 31 (1992) 9339–9349.
[7] J. Kihlberg, T. Fred, K. Jansson, and G. Magnusson, *Carbohydr. Res.*, 152 (1986) 113–130.
[8] R.I. El-Sokkray, B.A. Silwanis, M.A. Nashed, and H. Paulsen, *Carbohydr. Res.*, 203 (1990) 319–323.
[9] J. Alais and S. David, *Carbohydr. Res.*, 201 (1990) 69–77.
[10] Discover 2.8 Program, Biosym Technol. Inc., San Diego, USA.
[11] M. Bernabé, A. Fernández-Mayoralas, J. Jiménez-Barbero, M. Martín-Lomas, and A. Rivera-Sagredo, *J. Chem. Soc., Perkin Trans. 2*, (1989) 1867–1873.
[12] A. Imberty, Y. Bourne, C. Cambillau, P. Rouge, and S. Perez, *Adv. Biophys. Chem.*, in press; Y. Bourne, P. Rouge, and C. Cambillau, *J. Biol. Chem.*, 267 (1992) 197–203.
[13] S.W. Homans, *Biochemistry*, 29 (1990) 9110–9118; S.W. Homans and M. Forster, *Glycobiology*, 2 (1992) 143–151.
[14] H.C. Siebert, G. Reuter, R. Schauer, C.W. von der Lieth, and J. Dabrowski, *Biochemistry*, 31 (1992) 6962–6971; A.E. Aulabaugh, R.C. Crouch, G.E. Martin, A. Ragouzeos, J.P. Shockcor, T.D. Spitzer, R.D. Farrant, B.D. Hudson, and J.C. Lindon, *Carbohydr. Res.*, 230 (1992) 201–212.
[15] K. Bock, *Pure Appl. Chem.*, 55 (1983) 605–622; B. Meyer, *Top. Curr. Chem.*, 154 (1990) 141–208.
[16] K. Bock. H. Lönn, and T. Peters, *Carbohydr. Res.*, 198 (1990) 375–380.
[17] A. Rivera-Sagredo, J. Jiménez-Barbero, and M. Martín-Lomas, *Carbohydr. Res.*, 221 (1991) 37–47.
[18] Y. Nishida, H. Ohrui, and H. Meguro, *Tetrahedron Lett.*, 25 (1984) 1575–1578; D.M. Mackie, A. Maradufu, and A.S. Perlin, *Carbohydr. Res.*, 150 (1986) 23–33.
[19] Y. Nishida, H. Hori, H. Ohrui, and H. Meguro, *J. Carbohydr. Chem.*, 7 (1988) 239–250.
[20] C.A.G. Haasnoot, F.M. de Leeuw, and C. Altona, *Tetrahedron*, 36 (1980) 2783–2792.
[21] K. Bock and S. Refn, *Acta Chem. Scand., Ser. B*, 41 (1987) 469–472.
[22] L.M.J. Kroon-Batenburg and J. Kroon, *Biopolymers*, 29 (1990) 1243–1248.
[23] P. Fernández and J. Jiménez-Barbero, *Carbohydr. Res.*, 248 (1993) 15–36.
[24] G.W. Vuister, R. Boelens, and R. Kaptein, *J. Magn. Reson.*, 80 (1988) 176–182.
[25] D. Neuhaus and M.P. Williamson, *The Nuclear Overhauser Effect in Structural and Conformational Analysis*, VCH, New York, USA, 1989.

[26] M. Forster, C. Jones, and B. Mulloy, *J. Mol. Graph.*, 7 (1989) 196–201; M.J. Forster, *J. Comput. Chem.*, 12 (1991) 292–300. The program is now available through the Quantum Chemical Program Exchange, Indiana University, Bloomington, Illinois, USA, as QCPE 636.
[27] T. Peters, J.R. Brisson, and D.R. Bundle, *Can. J. Chem.*, 68 (1990) 979–988, and references therein.
[28] J.R. Brisson and J.P. Carver, *Biochemistry*, 22 (1983) 1362–1368; D.A. Cumming and J.P. Carver, *ibid.*, 26 (1987) 6664–6676; K.E. Miller, C. Mukhopadhyay, P. Cagas, and C.A. Bush, *ibid.*, 31 (1992) 6703–6709.
[29] A. Imberty, V. Tran, and S. Perez, *J. Comput. Chem.*, 11 (1989) 205–216; P. Cagas and C.A. Bush, *Biopolymers*, 30 (1990) 1123–1138.
[30] M. Hricovini, R.N. Shah, and J.P. Carver, *Biochemistry*, 31 (1992) 10018–10023.
[31] B.R. Leeflang, J.F.G. Vliegenthart, L.M.J. Kroon-Batenburg, B. P. van Eijck, and J. Kroon, *Carbohydr. Res.*, 230 (1992) 41–61.
[32] L. Poppe, R. Stuike-Prill, B. Meyer, and H. van Halbeek, *J. Biomol. NMR*, 2 (1992) 109–136.
[33] N. Yamasaki, T. Hatakeyama, and G. Funatsu, *J. Biochem.*, 98 (1985) 1555–1560.
[34] J.P. Frénoy, E. Turpin, F. Emmanuel, and A. Alfsen, in T.C. Bog-Hansen and D.L.J. Freed (Eds.), *Lectins: Biology, Biochemistry, Clinical Biochemistry*, Vol. 6, Sigma Chemical Co., St. Louis, 1988, 285–289.
[35] R.J. Youle, J.G. Murray, and D.M. Neville, *Cell*, 23 (1981) 551–559.
[36] D.J. States, D.J. Ruben, and R.A. Haberkorn, *J. Magn. Reson.*, 48 (1982) 286–291.
[37] A.T. Hagler, S. Lifson, and P. Dauber, *J. Am. Chem. Soc.*, 101 (1979) 5122–5130.
[38] S.J. Weiner, P.A. Kollman, D.A. Case, U.C. Singh, and C. Ghio, *J. Am. Chem. Soc.*, 106 (1984) 765–784.
[39] Insight 2.1.0 Program, Biosym Technol. Inc., San Diego, USA.
[40] G.L. Nicolson, J. Blaustein, and M.E. Etzler, *Biochemistry*, 13 (1974) 151–160.
[41] S.K. Podder, A. Surolia, and B.K. Bachhawat, *Eur. J. Biochem.*, 44 (1974) 151–160.